Iraqi Journal of Physics, 2024 *Vol. 22, No. 2, PP. 19-30*
https://doi.org/10.30723/ijp.v22i2.1216
P-ISSN: 2070-4003
E-ISSN: 2664-5548

Effect of Metal Oxides Nanoparticles on the Optical Properties of Poly(vinyl chloride)/Poly(vinylidene fluoride) Blends Electrolytes Plasticized with Glycerol

Russul Alaa Hasson[1a*] and Ahmad Abbas Hasan[1b]
[1]*Department of Physics, College of Science, University of Baghdad, Baghdad, Iraq*
[b]E-mail: ahmadabhasan2000@gmail.com
[a*]Corresponding author: rusal.alaa1604a@sc.uobaghdad.edu.iq

Abstract

Lithium-ion batteries (LIBs) are beginning to use solid polymer electrolytes (SPEs) as a potentially useful replacement for liquid electrolytes. However, incompatibility between the lithium metal anode and electrolyte, which results in low ionic conductivity and reduced cycling performance of LIBs, is one of the disadvantages of SPEs. Solution casting with glycerol as a plasticizer was used to create electrolyte films consisting of 80% Poly (vinylidene fluoride) (PVDF) and 20% poly (vinyl chloride) (PVC), undoped and doped with various salts, including lithium carbonate (Li_2CO_3) and lithium chloride (LiCl) and various metal oxides (CuO, WO_3, and TiO_2) nanoparticles (NPs). An investigation was conducted to examine their impact on optical properties. The prepared SPEs were characterized by UV-visible and Fourier transformer infrared spectroscopy (FTIR). The results showed that the type of salt and doping greatly affected the energy gap. The energy showed a blue shift after the addition of lithium carbonate, while it showed a red shift after doping with metal oxides (WO_3 and TiO_2) NPs; the minimum energy gap was 1.6 eV obtained from SPE (PVC/PVDF/Li_2CO_3) doped with TiO_2 NPs, while the energy gap showed red shift after adding LiCl. It changed non-regularly after doping with metal oxide NPs, reaching the lowest value of 1.8 eV for samples doped with WO_3 NPs. All optical constants were determined, and a graph of their values vs. wavelength was created. The FTIR analysis confirmed the presence of metal oxide NPs.

Article Info.

Keywords:
Solid Polymers Electrolytes, Glycerol, Metal Oxides, Lithium Carbonate, Lithium Chloride.

Article history:
Received: Nov. 05, 2024
Revised: Feb. 29, 2024
Accepted: Mar. 03, 2024
Published: Jun. 01, 2024

1. Introduction

Polymer electrolytes (PEs) are extensively studied due to their many electrical and battery uses [1]. In recent years, Lithium-Ion Batteries (LIBs) have received much attention in electrochemical energy storage systems because of their excellent characteristics, including their high energy density, single-cell voltage, and longer lifespan. LIBs are commonly found in smart grids, portable electronics, and hybrid and electric cars [2, 3]. Using the amorphous linear thermoplastic polymer poly (vinyl chloride) (PVC) has several industrial and medical uses, such as in manufacturing cannulas, catheters, and dialysis tubing sets [4]. It is readily available and has unique properties. Poly (vinylidene fluoride) (PVDF) polymer has many ideal qualities, such as a large voltage window, a long-term working temperature of up to 150^{o}C, a decomposition temperature of up to 400^{o}C, good electrochemical stability, and no adverse effects with other materials. With the PVDF's properties, high-quality, long-lasting PEs can be made. Polymer-ceramic composite electrolytes have been studied using lithium salts like LiCl and Li_2CO_3 [5]. Lithium salts form stable solid-electrolyte interphases due to their solubility and electrochemical stability [6].

Tsunemi et al. examined how plasticizers and lithium salts influenced electrolytes [7]. Inorganic filler limits the development of lithium dendrite formation [8]. according

to Liu et al. [9], polymer and inorganic filler interacted with Li dendrites. The reduced crystallinity and glass transition temperature (T_g) of the polymer phase generated by inorganic fillers increase conductive amorphous areas and segmental motion, which increases ionic conductivity [10-12]. Copper metal oxide (CuO) and tungsten trioxide (WO3) nanoparticles (NPs) improve PE stability and SPE oxidation resistance. CuO expands SPEs' electrochemical stability window and voltage stability range, which is useful in high-voltage batteries. Titanium dioxide (TiO_2) is widely investigated due to its unusual shape and surface properties. Its unique features include excellent photocatalytic activity, chemical stability, and refractive index.

Elashmawi et al. reported using a sonicator to prepare nanocomposites based on a PVDF/PVC blend containing graphene oxide nanoparticles (GO) [13]. The study revealed, from UV data, a decrease in the activation energy gap with increasing the GO content, implying a variation in reactivity due to reaction extent.

This work tested SPE matrix and PVC/PVDF polymer films with Li_2CO_3 and LiCl salts, CuO, WO3, and TiO_2 nanofillers using glycerol as a plasticizer [14]. It investigated the effect of the lithium salts and the metal oxide nanoparticles on the PVC/PVDF blend's optical properties and FTIR spectrum.

2. Experimental Work

The basic materials used in this work were PVC (supplied by SABIC Company, Saudi Arabia), PVDF, LiCl salt, Li_2CO_3 salt, CuO NPs, WO_3NPs, TiO_2NPs, glycerol (99% purity), and tetrahydrofuran (THF), all supplied by Sigma-Aldrich.

The solution casting method was used to create the electrolyte-thin films. A blend solution was prepared by dissolving 20% PVC and 80% PVDF in THF. After complete dissolution, the PVC/PVDF blend was doped with 10% lithium salts (LiCl and Li_2CO_3), to which 3 ml of plasticizer (glycerol) was added with continuous stirring until a homogeneous, viscous liquid was obtained. 0.01% metal oxide nanoparticles (CuO, WO_3, TiO_2) dissolved in THF were added to the lithium salts doped PVC/PVDF blends.

The blend solutions were poured into Petri dishes to evaporate the solvent at room temperature. The thickness of the freestanding films was measured with a micrometer to be 0.03 mm. The samples were dried in a vacuum at 60^{o}C for 24 hrs to get rid of any THF present.

A UV-visible spectrophotometer (UV-1800, Shimadzu, Japan) in the range of 190–1100 nm was used to measure the sample's UV or visible light absorption. The samples' infrared spectra were obtained with a Fourier transform infrared (FTIR) spectrometer (8400S, Shimadzu, Japan) in the 400–4000 cm^{-1} wavenumber range.

The electronic transitions of molecules affect UV-visible light absorption, which can reveal the sample's composition and concentration. For light of intensity of (I_o) passing through a sample, light intensity (I) passes out of the sample, according to [15]:

$$I = I_o e^{-\alpha t} \quad (\mathbf{1})$$

where t is the sample thickness and α is the absorption coefficient. Beer–Lambert's formula estimates the absorption coefficient as [16, 17]:

$$\alpha(\lambda) = 2.303\frac{A}{t} \quad (\mathbf{2})$$

where: A is the absorbance of a sample.

The Tauc equation links photon energy (hυ), absorption coefficient, and optical energy gap (E_g) as in the following relation [18]:

$$(\alpha h\upsilon) = \beta(h\upsilon - E_g)^r \quad (3)$$

where: β is a constant, r varies depending on the nature of the electron transition (r=0.5 for direct allowed, r=3/2 for forbidden, and r=2,3 for indirect transition).

The refractive index (n) is calculated by the following equation [19]:

$$n = \sqrt{\frac{(1+k)^2}{(1-k)^2} - (k^2 - 1)} + \frac{(1+R)}{(1-R)} \quad (4)$$

where: R is the reflectance of a material, and k is the extinction coefficient which quantifies the material's energy loss due to light scattering, according to [20]:

$$k = \frac{\alpha\lambda}{4\pi} \quad (5)$$

where: λ is the wavelength. ε_r and ε_i represent the real and imaginary parts of the dielectric constant, which are defined according to the following relations [21, 22]:

$$\varepsilon = \varepsilon_r - i\,\varepsilon_i \quad (6)$$

$$\varepsilon_r = n^2 - k^2 \quad (7)$$

3. Results and Discussion

3.1. Optical Properties

Figs. 1 and 2 show the absorbance spectra of PVC/PVDF blends doped with the two lithium salts (Li_2CO_3 and LiCl) and nanofillers (CuO, WO_3, and TiO_2) NPs. As the wavelength (λ) increased, the absorbance spectra PVC/PVDF, PVC/PVDF/Li_2CO_3, and PVC/PVDF/LiCl films decreased. Adding the metal oxides nanofillers increased the absorption, indicating component reactions. This result is confirmed by a previous study by Heiba et al. [23].

Figs. 3 and 4 show the transmittance of undoped and doped (PVC/PVDF/Li_2CO_3) and (PVC/PVDF/LiCl) blends and those with the nanofillers.

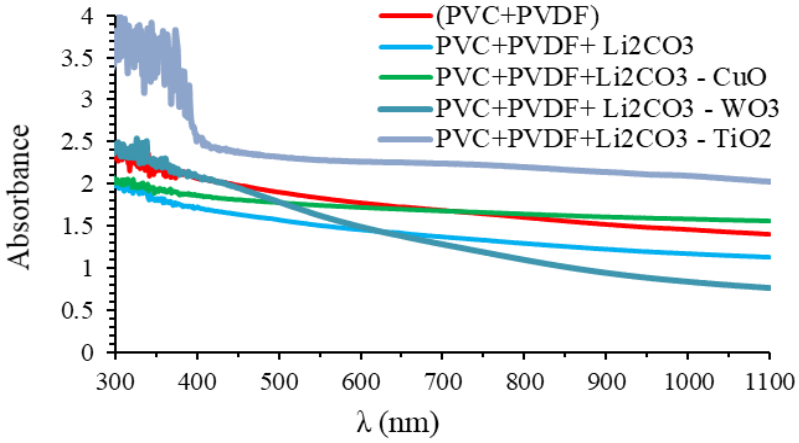

Figure 1: The absorbance as a function of λ for undoped and doped (PVC/PVDF/Li_2CO_3) blends with metal oxides nanoparticles.

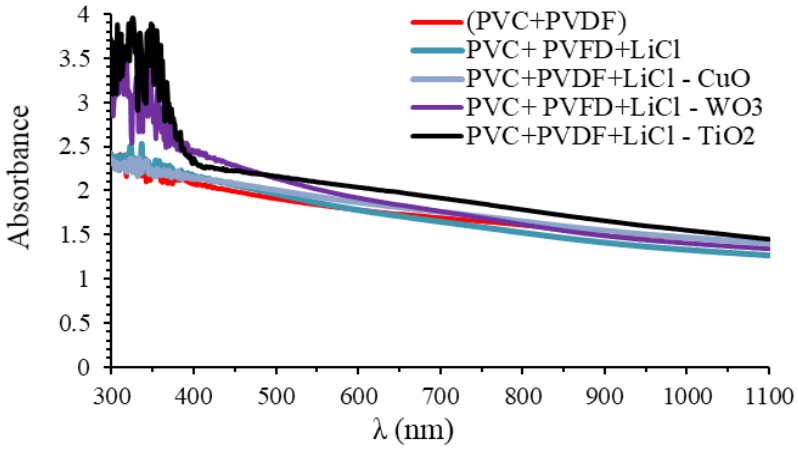

Figure 2: The absorbance as a function of λ for undoped and doped (PVC/PVDF/LiCl) blends with metal oxides nanoparticles.

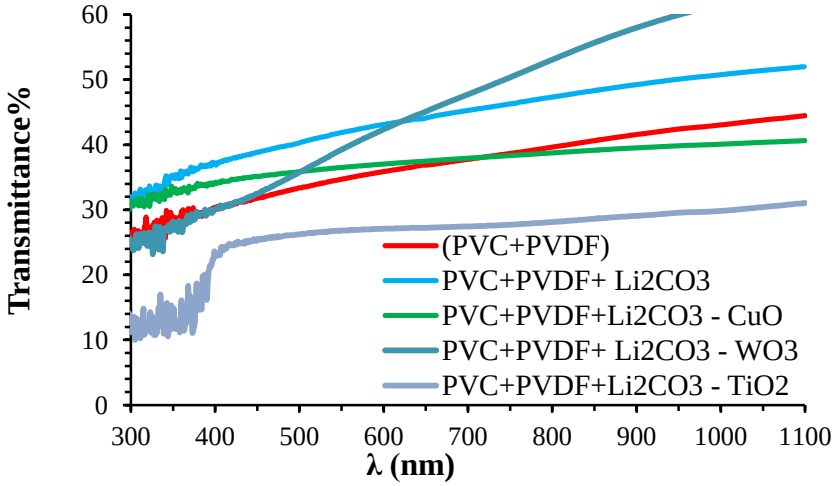

Figure 3: The transmittance as a function of λ for undoped and doped (PVC/PVDF/Li_2CO_3) blends with metal oxides nanoparticles.

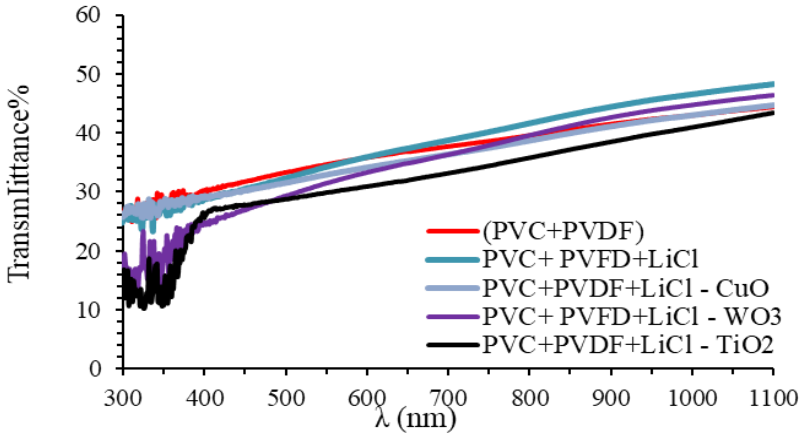

Figure 4: The transmittance as a function of λ for undoped and doped (PVC/PVDF/LiCl) blends with metal oxides nanoparticles.

Optical band gap energy (E_g) was calculated by plotting $(\alpha h\upsilon)^2$ versus ($h\upsilon$), as shown in Figs. 5 and 6 for the synthesized undoped (PVC/PVDF/Li_2CO_3,LiCl) and doped with different metal oxide NPs, where E_g is the photon energy intercept at zero absorption coefficient. The direct optical energy gap of the PVC/PVDF blend was 2.2 eV, as shown in Table 1. Adding different lithium salts, E_g rose to 2.25 eV for Li_2CO_3 and fell to 1.95 eV for LiCl.

A study by Rajesh et al. reported that the optical band gap energy decreased with the addition of TiO_2 nanoparticles [24]. As noted in Table 1, the optical band gap energy of (PVC/PVDF/Li_2CO_3) decreased with doping with NPs metal oxides, reaching 1.6 eV for TiO_2. Band gap energies of (PVC/PVDF/LiCl) blends, and those doped with nanofillers showed irregular changes.

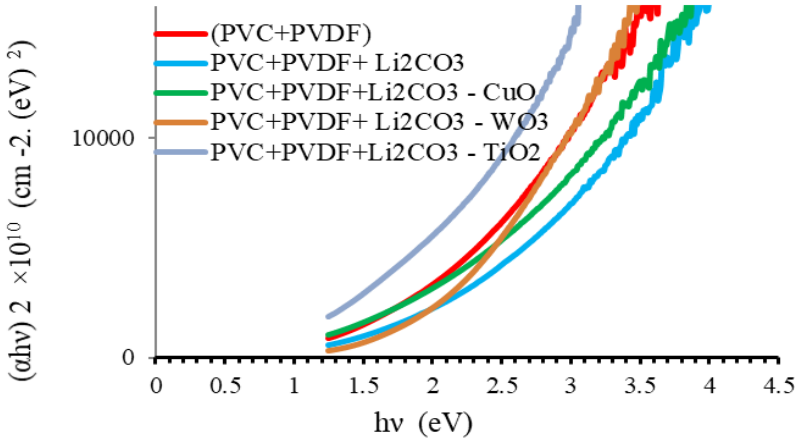

Figure 5: $(\alpha h\upsilon)^2$ versus ($h\upsilon$) for undoped and doped (PVC/PVDF/Li_2CO_3) blends with metal oxides nanoparticles.

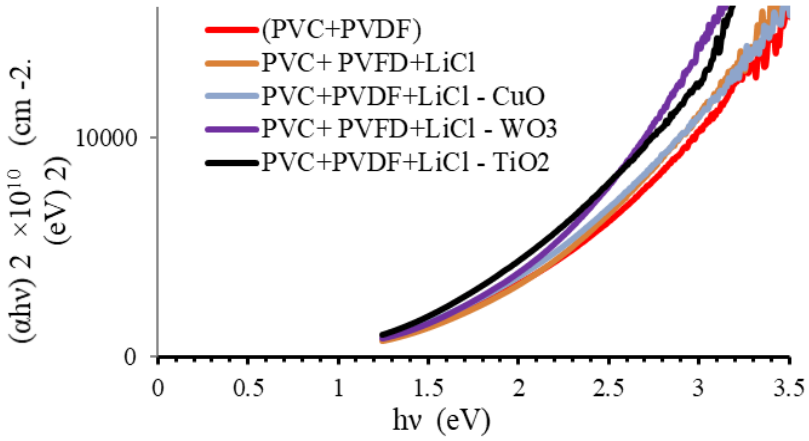

Figure 6: $(\alpha h\upsilon)^2$ versus ($h\upsilon$) for undoped and doped (PVC/PVDF/LiCl) blends with metal oxides.

Figs. 7 and 8 show the relation of the refractive index (n) of undoped (PVC/PVDF/Li_2CO_3, LiCl) blends and doped with different metal oxide NPs with wavelength. The refractive index of (PVC/PVDF/LiCl) blend and the blends doped with the different metal oxide NPs were less than that of (PVC/PVDF), but they were higher for (PVC/ PVFD/Li_2CO_3) blend and for the blends doped with the different metal oxide

NPs. Khudher et al. reported that the increase in the refractive index is related to the increase in packing density (the material becoming opaque), which causes the velocity of light in the medium to decrease [25]. In this study, adding Li_2CO_3 and doping with metal oxides NPs made the sample opaque, decreasing lowering light propagation velocity and raising the n values. However, adding LiCl and doping with metal oxides NPs made the samples less dense (more transparent to incident light), which increased light velocity through the samples, thus lowering the refractive index value [26].

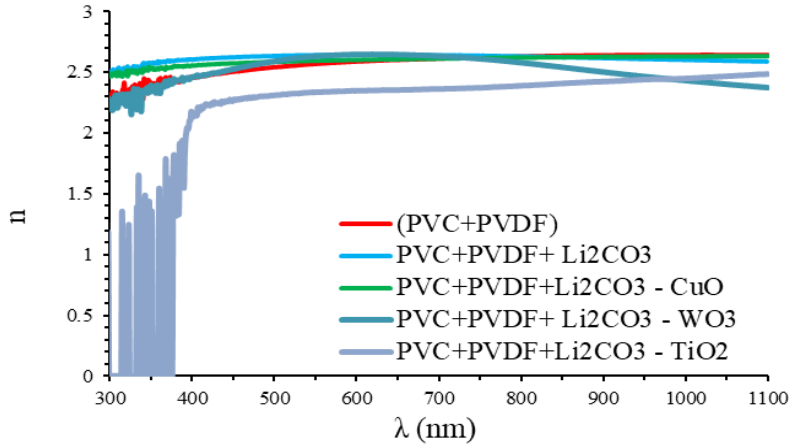

Figure 7: The refractive index as a function of λ for undoped and doped PVC/PVDF/Li_2CO_3) blends with metal oxides nanoparticles.

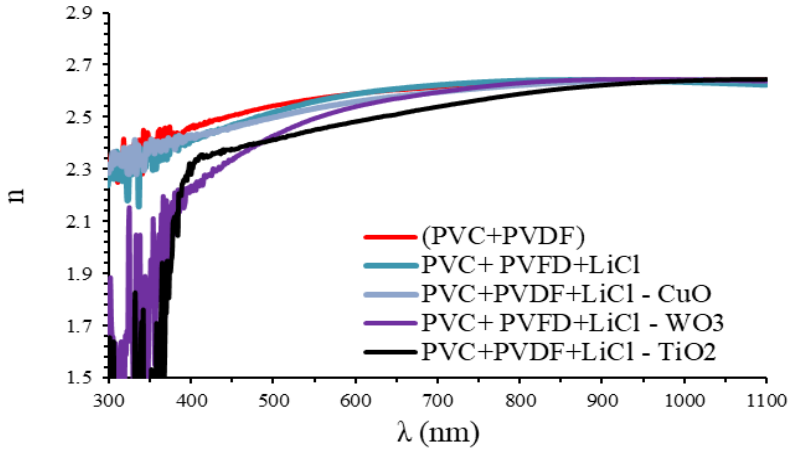

Figure 8: The refractive index as a function of λ for undoped and doped (PVC/PVDF/LiCl) blends with metal oxides nanoparticles.

The changes of the extinction coefficient for the different blends are shown in Figs. 9 and 10. When CuONPs and WO_3NPs were added to the PVC/PVDF/Li_2CO_3 mix, the extinction coefficient (k) value went down from $1.32x10^{-4}$ to $1.26x10^{-4}$ and then to $1.17x10^{-4}$. The incorporation of TiO_2NPs into the mixture led to a significant enhancement, as illustrated in Table 1. The undoped blend of poly (vinyl chloride) and poly (vinylidene fluoride) with lithium chloride has an extinction value of 1.32×10^{-4}. The inclusion of lithium chloride and the introduction of CuONPs, WO_3NPs, and TiO_2NPs through doping led to an augmentation in the extinction coefficient. More precisely, the inclusion of LiCl salt resulted in an elevation of the extinction coefficient

to $1.39x10^{-4}$, $1.45x10^{-4}$, and $1.51x10^{-4}$ for CuONPs, WO_3NPs, and TiO_2NPs, respectively.

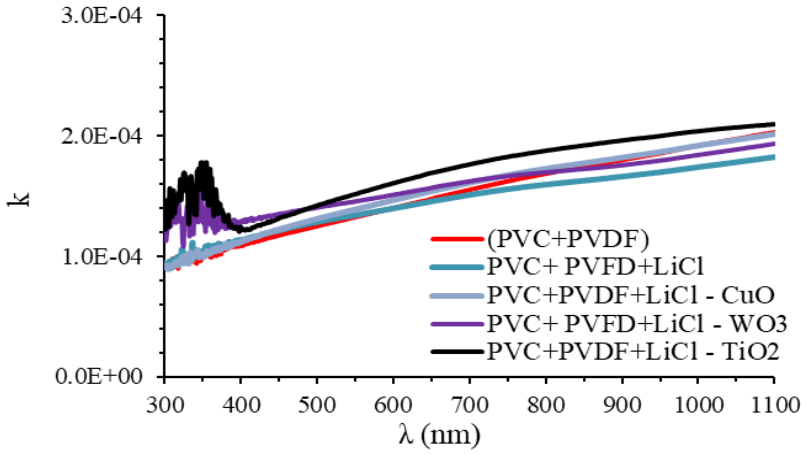

Figure 9: The extinction coefficient as a function of λ for undoped and doped (PVC/PVDF/LiCl) blends with metal oxides.

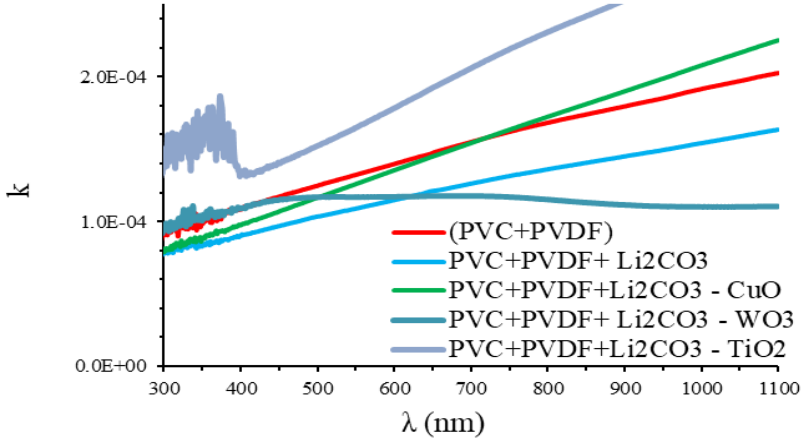

Figure 10: The extinction coefficient as a function of λ for undoped and doped (PVC/PVDF/Li_2CO_3) blends with metal oxides.

In Figs. 11-14, the real and imaginary dielectric constants of undoped PVC/PVDF/Li_2CO_3, LiCl blends and doped with metal oxides nanoparticles are plotted as a function of wavelength. The real dielectric constant of PVC/PVDF/Li_2CO_3 exhibited a notable rise in the presence of Li_2CO_3 salt, but it experienced a drop upon doping with different metal oxide nanoparticles. The lowest value was actually recorded in the PVC/PVDF/Li_2CO_3 sample that was doped with TiO_2. Rajesh et al. reported that the dielectric constant increased up to 12 wt.% doping of TiO_2 and therefore the increase in the doping concentration reduced the dielectric constant [24]. The inclusion of LiCl and doping both resulted in a systematic decrease in the real dielectric constant of PVC/PVDF/LiCl blends. The inclusion of Li_2CO_3 results in a decrease in the imaginary dielectric constant of PVC/PVDF/Li_2CO_3 blends, reducing it from 6.18×10^{-4} to 5.76×10^{-4}. The dielectric constant exhibits erratic fluctuations when doped with various metal oxide nanoparticles. Incorporating LiCl and introducing metal oxide

nanoparticles as dopants results in an increase of the imaginary dielectric constant in PVC/PVDF/LiCl blends [27].

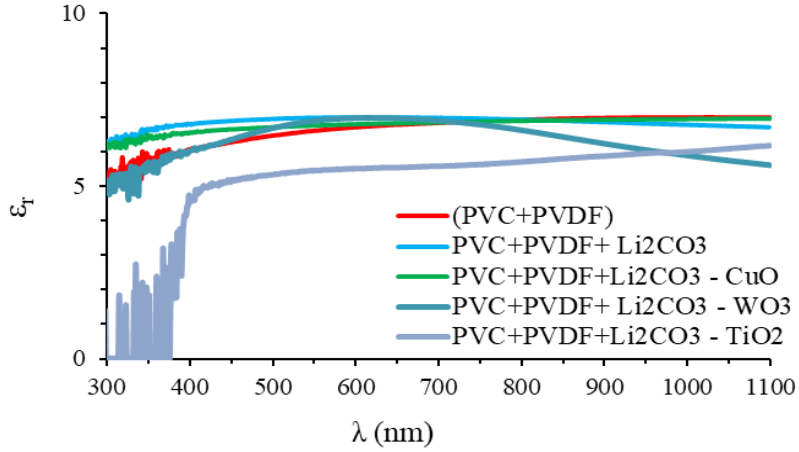

Figure 11: The real (ε_r) dielectric constant as a function of λ for undoped and doped (PVC/PVDF/Li_2CO_3) blends with metal oxides nanoparticles.

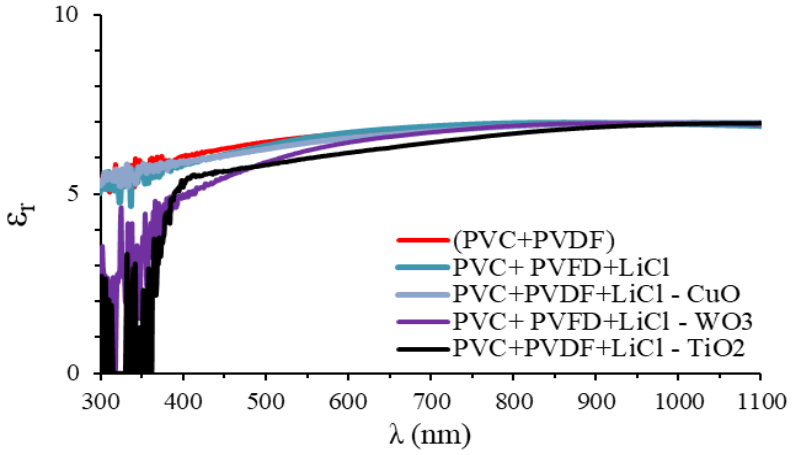

Figure 12: The real (ε_r) dielectric constant as a function of λ for undoped and doped (PVC/PVDF/LiCl) blends with metal oxides nanoparticles.

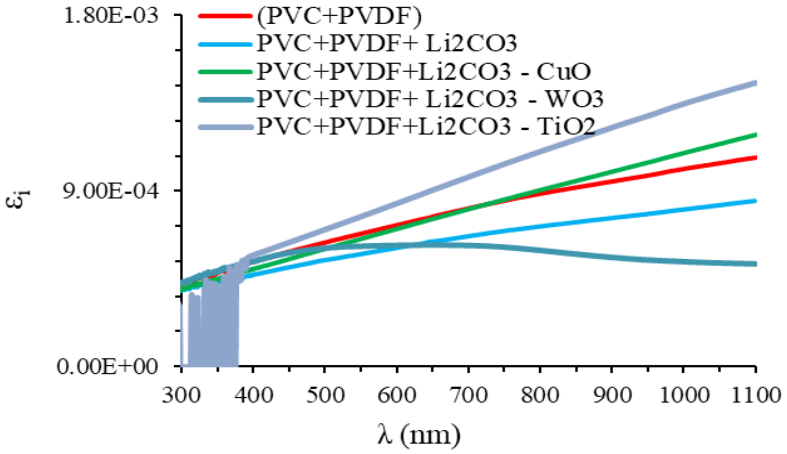

Figure 13: The imaginary (ε_i) dielectric constant as a function of λ for undoped and doped (PVC/PVDF/Li_2CO_3) blends with metal oxides nanoparticles.

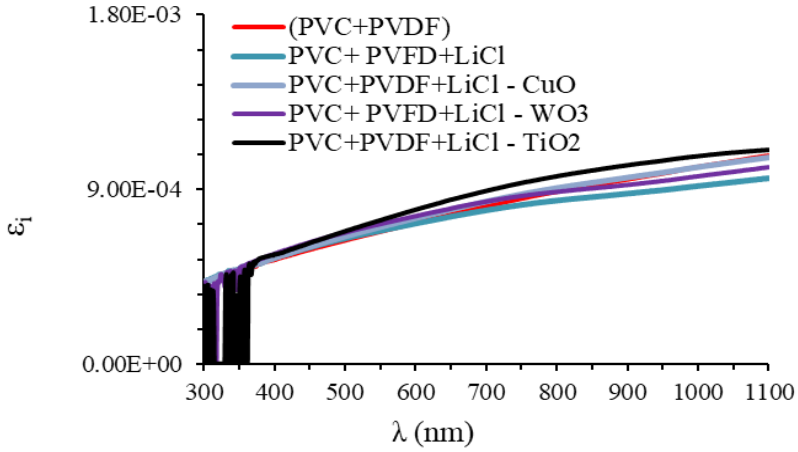

Figure 14: The imaginary (ε_i) dielectric constant as a function of λ for undoped and doped (PVC/PVDF/LiCl) blends with metal oxides nanoparticles.

Table 1: Values of optical parameters constant at λ=550nm of PVC/PVDF, PVC/PVDF/Li_2CO_3 and PVC/PVDF/LiCl blends and doped with CuO, WO_3 and TiO_2NPs.

Sample	T%	α	k	n	ε_r	ε_i	E_g (eV)
PVC/PVDF	34.69	30	$1.32x10^{-4}$	2.569	6.602	$6.81x10^{-4}$	2.2
PVC/ PVFD/Li_2CO_3	41.86	25	$1.09x10^{-4}$	2.641	6.977	$5.76x10^{-4}$	2.25
PVC/PVDF/Li_2CO_3-CuO	36.52	29	$1.26x10^{-4}$	2.599	6.752	$6.55x10^{-4}$	2.24
PVC/PVDF/Li_2CO_3-WO_3	39.24	27	$1.17x10^{-4}$	2.628	6.905	$6.15x10^{-4}$	1.9
PVC/PVDF/Li_2CO_3-TiO_2	26.81	38	$1.65x10^{-4}$	2.335	5.450	$7.69x10^{-4}$	1.6
PVC/PVFD/LiCl	34.28	31	$1.34x10^{-4}$	2.562	6.561	$6.86x10^{-4}$	1.95
PVC/PVDF/LiCl-CuO	32.96	32	$1.39x10^{-4}$	2.534	6.420	$7.04x10^{-4}$	2
PVC/PVDF/LiCl-WO_3	31.41	33	$1.45x10^{-4}$	2.495	6.224	$7.23x10^{-4}$	1.8
PVC/PVDF/LiCl-TiO_2	29.91	34	$1.51x10^{-4}$	2.450	6.004	$7.40x10^{-4}$	2.8

3.2. Fourier Transform Infrared spectroscopy (FTIR)

Fig. 15 shows the FTIR spectra of the various blends undoped and doped with metal oxides nanoparticles in the wavenumber range of 4000-500 cm^{-1}. Lithium salts and metal oxides are present in the PVC/PVDF blends at 4000-500 cm^{-1}. A strong and wide absorption peak at 3336 cm^{-1} is due to the high hydrogen bonding in OH stretching [28]. This peak shifts to (3371, 2256, 3313, 3363, 3360, 3321, and 3367) cm^{-1}. As shown by the line broadening, chemical groups can be connected intramolecularly or intermolecularly [29]. The C-H stretch for sp3-hybridized carbon atoms was at 2881 and 2935 cm^{-1}. Stretching C=C caused the 1654 cm^{-1} absorption peak. C-F bonds were located at (1404, 1192, 1111, 991, 875, 763, 675, 486) cm^{-1}. The peak at 1041 cm^{-1} is related to C-H bending vibration. PVDF's C-F stretching vibration peak was around 1000 cm^{-1} [30]. The 559 cm^{-1} bond may be due to the PVC's C-Cl stretching vibration [31]. The absorption peak indicated chlorine atoms in the PVC polymer chain. The oxygen atoms of the carbonate ion stretch within the Li_2CO_3 molecule, demonstrating their vibrational movements at 918 and 1450 cm^{-1}, respectively. At 921 and 1458 cm^{-1}, the Cl-Li-Cl bond angle's vibrational bending matched the absorption band.

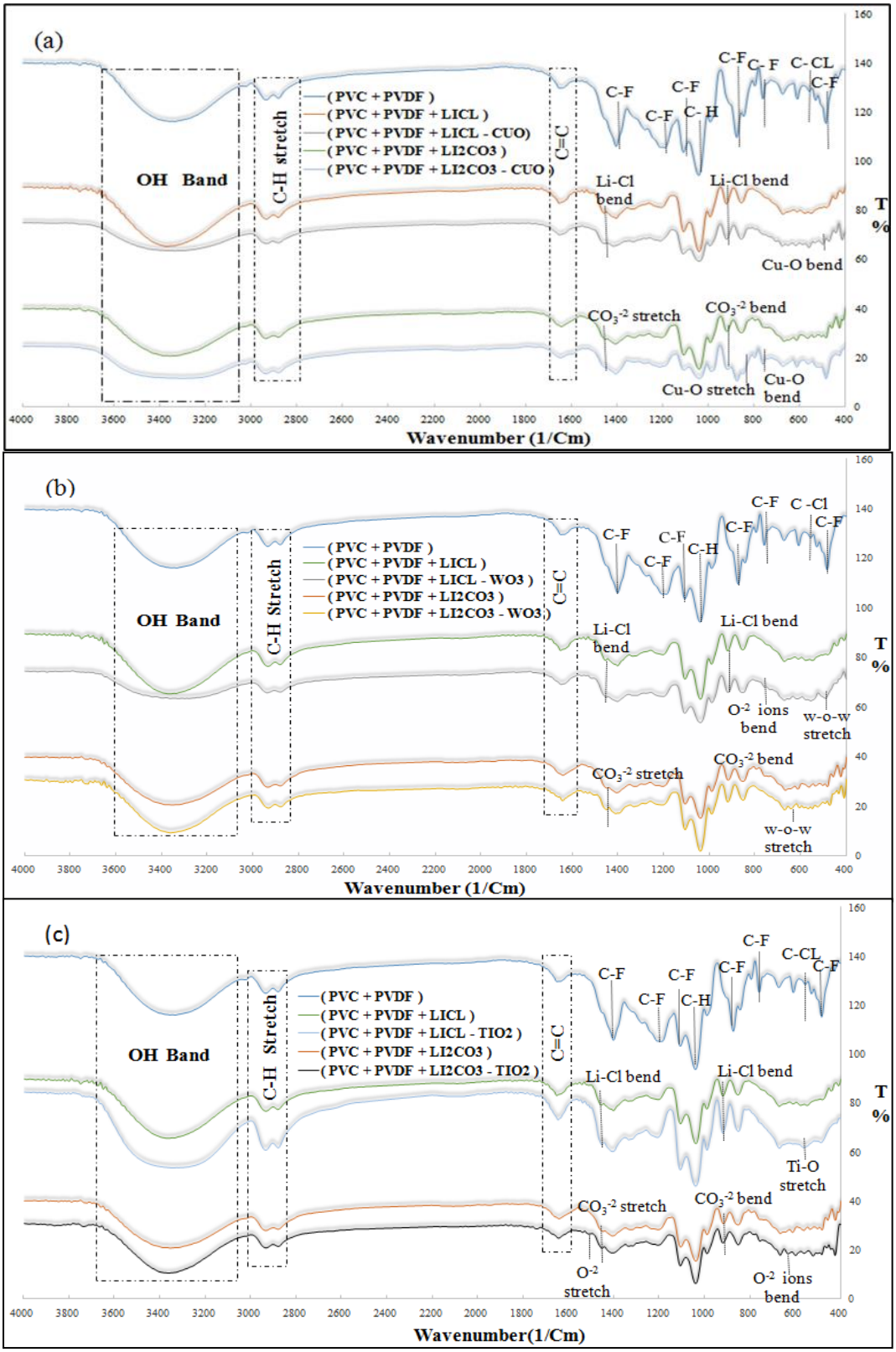

Figure 16: FTIR of (a)(PVC/PVDF/LiCl, Li_2CO_3) doped with CuO nanoparticles (b) (PVC/PVDF/LiCl, Li_2CO_3) doped with WO_3 nanoparticles (c) (PVC/PVDF/LiCl, Li_2CO_3) doped with TiO_2 nanoparticles.

After adding CuONPs, the fingerprint peaks changed in strength. PVC/PVDF/LiCl/CuO showed a Cu-O bond bending vibration at 497 cm^{-1}. PVC/PVDF/Li_2CO_3/CuO showed a bending vibration at 759 cm^{-1}, indicating oxygen in its atom and a stretching vibration at 848 cm^{-1}. WO_3 stretched the W-O-W bonds in

(PVC/PVDF/LiCl, Li_2CO_3/WO_3) mix. The PVC/PVDF/LiCl/TiO_2 blend showed Ti-O bond stretching vibration at 567 cm^{-1}. While (PVC/PVDF/Li_2CO_3/TiO_2) demonstrated oxygen atom bending and stretching vibrations at 636 and 1509 cm^{-1} in the TiO_2 lattice. Elashmawi et al. showed that the intensities of the α-phase PVDF bands for PVC/PVDF blend doped with graphene oxide nanoparticles decreased with increasing graphene oxide content [13].

5. Conclusions

Solution casting resulted in 20% PVC+80% PVDF blends complexed with 10% Li_2CO_3 and LiCl salts, doped with CuO, WO_3, and TiO_2 NPs, and plasticized with glycerol. Localized band gap states of LiCl salts reduced the energy gap. The optical band gaps got smaller when CuO and WO_3 nanofillers were added along with LiCl salts. This makes them a favorable choice for improving electrical properties when doping with TiO2, as it broadens the energy gap. The PVC/PVDF/Li_2CO_3 doped with TiO_2NPs achieved a minimum E_g value of 1.6 eV. Adding CuO, WO_3, and TiO_2 NPs affected the dielectric constant and dielectric loss. The maximum values for the dielectric constant and dielectric loss of the PVC/PVDF/LiCl/WO_3 blend were 1618.833 and 541.3477, respectively. The addition of CuO, WO_3, and TiO_2 NPs to the PVC/PVDF blend confirmed the chemical composition and structure of the blend, as revealed by FTIR measurements. The suggestion is to look into what happens to the mechanical properties when metal oxides are added and how ionization radiation changes the optical and electrical properties of PVC/PVDF blends that have not been doped but have been doped with different lithium salts.

Acknowledgements

The authors would like to thank the University of Baghdad, College of Science, Department of Physics, for their assistance in carrying out this work.

Conflict of interest

Authors declare that they have no conflict of interest.

References

1. M. H. Rahman, H. Werth, A. Goldman, Y. Hida, C. Diesner, L. Lane, and P. L. Menezes, Ceramics **4**, 516 (2021).
2. D. Zhou, D. Shanmukaraj, A. Tkacheva, M. Armand, and G. Wang, Chem **5**, 2326 (2019).
3. X. Zhang, S. Wang, C. Xue, C. Xin, Y. Lin, Y. Shen, L. Li, and C. W. Nan, Advan. Mater. **31**, 1806082 (2019).
4. S. T. Gaballah, H. A. El-Nazer, R. A. Abdel-Monem, M. A. El-Liethy, B. A. Hemdan, and S. T. Rabie, Int. J. Bio. Macromolec. **121**, 707 (2019).
5. D. Das and S. Samanta, ACS Appl. Elect. Mater. **3**, 1634 (2021).
6. X. Yu and A. Manthiram, En. Stor. Mater. **34**, 282 (2021).
7. K. Tsunemi, H. Ohno, and E. Tsuchida, Electrochim. Act. **28**, 833 (1983).
8. F. Ye, X. Zhang, K. Liao, Q. Lu, X. Zou, R. Ran, W. Zhou, Y. Zhong, and Z. Shao, J. Mater. Chem. A **8**, 9733 (2020).
9. R. Liu, Z. Wu, P. He, H. Fan, Z. Huang, L. Zhang, X. Chang, H. Liu, C.-A. Wang, and Y. Li, J. Materiom. **5**, 185 (2019).
10. Z. Lv, Q. Zhou, S. Zhang, S. Dong, Q. Wang, L. Huang, K. Chen, and G. Cui, En. Stor. Mater. **37**, 215 (2021).
11. H. He, Y. Chai, X. Zhang, P. Shi, J. Fan, Q. Xu, and Y. Min, J. Mater. Chem. A **9**, 9214 (2021).

12. J. Fu, Z. Li, X. Zhou, and X. Guo, Mater. Advan. **3**, 3809 (2022).
13. I. Elashmawi, N. S. Alatawi, and N. H. Elsayed, Res. Phys. **7**, 636 (2017).
14. M. A. Brza, S. B. Aziz, H. Anuar, S. M. Alshehri, F. Ali, T. Ahamad, and J. M. Hadi, Membranes **11**, 296 (2021).
15. S. Raghavendra, S. Khasim, M. Revanasiddappa, M. Ambika Prasad, and A. Kulkarni, Bull. of Mat. Sci. **26**, 733 (2003).
16. P. A. Kyriacou and J. Allen, *Photoplethysmography: Technology, Signal Analysis and Applications* (London, UK, Academic Press, 2021).
17. R. Luo, Y. Wu, Q. Li, B. Du, S. Zhou, and H. Li, Synth. Met. **274**, 116720 (2021).
18. P. Jubu, F. Yam, V. Igba, and K. Beh, J. Sol. St. Chem. **290**, 121576 (2020).
19. B. A. Hasan and M. A. Kadhim, AIP Conference Proceedings (Karbala, Iraq AIP Publishing, 2019). p. 030021.
20. A. Hazim, A. Hashim, and H. Abduljalil, Egyptian J. Chem. **64**, 359 (2021).
21. E. Abou Hussein, M. A. Maksoud, R. A. Fahim, and A. Awed, Opt. Mater. **114**, 111007 (2021).
22. H. Alfannakh, Advan. Mater. Sci. Eng. **2022**, 1 (2022).
23. Z. K. Heiba, A. El-Naggar, M. B. Mohamed, A. Kamal, M. Osman, A. Albassam, and G. Lakshminarayana, Opt. Mater. **122**, 111788 (2021).
24. K. Rajesh, V. Crasta, N. Rithin Kumar, G. Shetty, and P. Rekha, J. Poly. Res. **26**, 99 (2019).
25. R. H. Khudher and A. A. Hasan, PAN **200**, 225 (2022).
26. B. A. Hasan, S. S. Mahmood, H. H. Issa, and T. T. Issa, AIP Conference Proceedings (AIP Publishing, 2021). p. 040010
27. B. A. Hasan and M. A. Kadhim, IOP Conference Series: Materials Science and Engineering (Thi-Qar, Iraq IOP Publishing, 2020). p. 072009.
28. S. B. Aziz, M. M. Nofal, R. T. Abdulwahid, M. Kadir, J. M. Hadi, M. M. Hessien, W. O. Kareem, E. M. Dannoun, and S. R. Saeed, Res. Phys. **29**, 104770 (2021).
29. G. M. Ter Huurne, I. K. Voets, A. R. Palmans, and E. Meijer, Macromolecules **51**, 8853 (2018).
30. Y. Qi, L. Pan, L. Ma, P. Liao, J. Ge, D. Zhang, Q. Zheng, B. Yu, Y. Tang, and D. Sun, J. Mater. Sci. Mater. Elect. **24**, 1446 (2013).
31. D. Ma, L. Liang, E. Hu, H. Chen, D. Wang, C. He, and Q. Feng, Proce. Saf. Envir. Prot. **146**, 108 (2021).

تشخيص خلطات PVC/PVDF الالكتروليتية ذات الاساس البوليمري المطعمة بأكاسيد المعادن

رسل علاء حسون[1] واحمد عباس حسن[1]
[1] قسم الفيزياء، كلية العلوم، جامعة بغداد، بغداد، العراق

الخلاصة

تم استخدام طريقة صب المحلول مع الجلسرين كمادة ملدنة لتكوين أغشية الكتروليتية من (PVDF/PVC-Li_2CO_3, LiCl) غير المطعمة والمطعمة بالجسيمات النووية المختلفة من أكاسيد المعادن (CuO, WO_3, and TiO_2). تم تشخيص الالكتروليتات البوليمرية الصلبة بواسطة التحليل الطيفي للأشعة تحت الحمراء المرئية فوق البنفسجية و.FTIR أظهرت النتائج ان فجوة الطاقة تتأثر بشكل كبير بنوع الملح والمطعمات. أظهرت الطاقة تحولاً بعد اضافة كاربونات الليثيوم بينما اظهرت تحولاً ملحوظا بعد التطعيم بأكاسيد المعادن NPs (WO_3, TiO_2) وكان الحد الادنى لفجوة الطاقة 1.6 فولت تم الحصول عليها من PVC/PVDF/Li_2CO_3 المطعم ب TiO_2 NPs, بينما اظهرت الطاقة تحولاً ملحوظ بعد اضافة كلوريد الليثيوم ويتغير بطريقة غير منتظمة بعد التطعيم بالأكاسيد والتي تصل الى القيمة الأقل 1.8 فولت للعينة المطعمة ب WO_3 NPs. تم تحديد جميع الثوابت الضوئية وتم انشاء رسم بياني لقيمها مقابل الطول الموجي. وأكد تحليل FTIRوجود أكاسيد المعادن.

الكلمات المفتاحية: الالكتروليتات البوليمرية الصلبة، الجلسرين، الأكاسيد المعدنية، كاربونات الليثيوم، كلوريد الليثيوم.